J Mol Model (2012) 18:3379–3388
DOI 10.1007/s00894-011-1339-2

ORIGINAL PAPER

The solvation study of carbon, silicon and their mixed nanotubes in water solution

Haleh Hashemi Haeri · Sepideh Ketabi · Seyed Majid Hashemianzadeh

Received: 5 July 2011 / Accepted: 19 December 2011 / Published online: 21 January 2012

Abstract Nanotubes are believed to open the road toward different modern fields, either technological or biological. However, the applications of nanotubes have been badly impeded for the poor solubility in water which is especially essential for studies in the presence of living cells. Therefore, water soluble samples are in demand. Herein, the outcomes of Monte Carlo simulations of different sets of multiwall nanotubes immersed in water are reported. A number of multi wall nanotube samples, comprised of pure carbon, pure silicon and several mixtures of carbon and silicon are the subjects of study. The simulations are carried out in an (N,V,T) ensemble. The purpose of this report is to look at the effects of nanotube size (diameter) and nanotube type (pure carbon, pure silicon or a mixture of carbon and silicon) variation on solubility of multiwall nanotubes in terms of number of water molecules in shell volume. It is found that the solubility of the multi wall carbon nanotube samples is size independent, whereas multi wall silicon nanotube samples solubility varies with diameter of the inner tube. The higher solubility of samples containing silicon can be attributed to the larger atomic size of silicon atom which provides more direct contact with the water molecules. The other affecting factor is the bigger inter space (the space between inner and outer tube) in the case of silicon samples. Carbon type multi wall nanotubes appeared as better candidates for transporting water molecules through a multi wall nanotube structure, while in the case of water adsorption problems it is better to use multi wall silicon nanotubes or a mixture of multi wall carbon/silicon nanotubes.

Keywords Mixed nanotubes · Monte Carlo simulation · Multi wall carbon nanotubes · Multi wall silicon nanotubes · Nanotube dispersion · Solvation energies

H. Hashemi Haeri (✉) · S. Ketabi
Department of Chemistry, East Tehran Branch (Ghiamdasht), Islamic Azad University,
Tehran, Iran
e-mail: hashemihaeri@gmail.com

S. M. Hashemianzadeh
Molecular Simulation Research Laboratory, Departments of Chemistry, Iran University of Science and Technology (IUST),
Tehran, Iran

Introduction

Structurally well-defined building blocks are potentially useful in the synthesis of designed catalysts, photonic band gap materials, nanoscale electronic devices, and chemical separations media [1]. Tabular structures are particularly interesting in this regard, because of their inherent mechanical strength [2], their unusual electronic transport properties [3], and their ability to act as containers or capsules [4, 5].

Carbon nanotubes (CNTs), a new form of carbon, have come under intense multidisciplinary studies because of their unique physical and chemical properties [6, 7]. The well-defined shape and size of NTs make them attractive candidates for theoretical and experimental studies of various nanoscopic phenomena such as protection and confinement of molecular species as well as transport of molecules through their interior pores [8].

CNTs include single wall (SW) and multi wall (MW) depending on the number of layers comprising them [6]. As aforementioned, the unique properties of nano-tabular structures, including CNTs, have led to interest in their potential application as quantum nanowires, electron field emitters, catalyst supports, chemical sensors [9], and sorbents for hydrogen and other gas storages [4, 10–12]. In

addition to the aforesaid properties, one can mention the other properties of great importance such as large specific surface area, light mass density, hollow cavities, and excellent mechanical and electrical properties.

The development of new nanoscale platforms offers great potential for improvements in the care of cancer patients in the near future. Areas of greatest clinical impact likely include novel, targeted drug-delivery vehicles, molecularly targeted contrast agents for cancer imaging, targeted thermal tumor ablation, and magnetic field targeting of tumors [13, 14].

Although the interfacing CNTs with biological systems can lead to significant applications in various disease diagnoses, the toxicity of the nanotubes interacting with living cells is an issue of strong concern. However one can say that the data on the toxicity of CNTs from a biological perspective is poor or contradictory [15–22]. On the other hand, non-functionalized NTs are poorly soluble in water, organic or inorganic solvents. As a result, a lot of effort has been put into making soluble NTs, recently.

Solubilization methods of NTs are still controversial topics in contemporary NT literature [23, 24]. This behavior of NTs is commonly attributed to their long structured features, large molecular size, or severe aggregation [25]. CNTs can be solubilized by a series of methods, including their functionalization by the aryl diazonium process, use of elemental metals, simple inorganics, acids, esters, aldehydes, amines, aromatics, macrocycles, thiols, biomolecules, polymers, and using such techniques as pulsed streamer discharge, microwave treatment, cryogenic crushing [25].

Another method which has hardly been noticed as a way to make MWNTs soluble is doping method [25]. Experimentally, the first attempts to replace carbon atoms with silicon in fullerens were not successful. However, the partial substitution of carbon (C) atoms by silicon (Si) atoms which results in cohabitation is possible [26]. Indeed, SiC nanotubes (SiCNT) were first observed by Sun et al. [27] by a substantial reaction with Si replacing the C atoms in an MWNT structure. Mavrandonakis et al. studied the stability of such materials by DFT calculations. They found out that increasing Si over C ratio made SiCNTs instable, which was in agreement with Sun et al. findings. Referred to in these literature a 50% SiCNT is the best suggested structure in this category of mixed NTs [26]. In a very recent paper, Malek and Shahimi studied the effect of the NT's size, curvature, and chirality on diffusion and adsorption of several gases in SWSiCNTs by molecular dynamics (MD) simulations. They showed that adsorption sites in a NT with finite length favor hydrogen binding to the SWSiCNTs over the SWCNTs. Also, the adsorption capacity and diffusion of gases in the SiCNTs were strongly affected by the SiCNTs curvature and chirality [28].

As authors were very keen on the effect of doping on the solubility of MWNTs, a series of Monte Carlo (MC) simulations were conducted to study the solvation behavior of different kinds of MWNTs consisting of C and Si atoms. Both pure (consist of only C (MWCNT) or Si (MWSiNT) atoms) and mixed samples (comprised of both C and Si atoms) were examined. MWNTs were considered with different inner diameters while the outer tube diameter and MWNTs length were kept constant.

The remainder of this paper is organized as follows. The simulation setup and computational details are described in section 2. Then it is followed by the analysis of results in terms of solvation energies and diameter (size) effect in Sect. 3. Conclusions are drawn in Sect. 4.

Simulation setup

Calculated energy values, as well as various structural parameters, can be further used to analyze solvation energies of the NTs [29]. The process of solvation of the solute molecule (NTs) in water can be defined as follows:

$$\mathrm{NT(g)} \leftrightarrow \mathrm{NT(aq)}.$$

Total potential energy of a chemical system, ΔEtot, includes internal potential energy (ΔEint) and external potential energy (ΔEext) terms:

$$\Delta E_{tot} = \Delta E_{\mathrm{int}} + \Delta E_{ext} \tag{1}$$

ΔEtot can be further explained as the sum of the energy contributions from solute-solvent

(ΔEsoln), solvent-solvent (ΔEsolv), and intramolecular (ΔEint) interactions:

$$\Delta E_{tot} = \Delta E_{\mathrm{int}} + \Delta E_{so\,\mathrm{ln}} + \Delta E_{solv} \tag{2}$$

The canonical MC method at T=298 K was used to examine the solvation behavior of MWNT systems in water, applying the standard Metropolis sampling technique [30, 31]. The interaction between two molecules a and b were defined by a site-site interaction potential consisting of a standard Lennard-Jones (LJ) potential to represent the short range potential and a long range Coulomb potential, with parameters, εi , σi, and qi for each atom:

$$U_{ab} = \sum_{j\in a}\sum_{j\in b} 4\varepsilon ij\left[\left(\frac{\sigma_{ij}}{rij}\right)^{12} - \left(\frac{\sigma_{ij}}{r_{ij}}\right)^{6}\right] + \frac{q_i q_j e^2}{r_{ij}} \tag{3}$$

The transferable intermolecular potential functions [32, 33] (TIP3) was applied for modeling solvent molecules. This model uses a total of the three sites for the electrostatic interactions. The partial positive charges on the hydrogen atoms were exactly balanced by an appropriate negative charge located on the oxygen atom. The characteristics of the LJ parameters for C and Si [33–35] are given in Table 1.

The site-site LJ parameters for the unlike interactions,εCO ,σCO, εCH ,σCH, εOH ,σOH, were obtained according to the standard Lorenz-Berthelot (LB) combining rule [36],

$$\sigma_{ij} = \frac{1}{2}\left(\sigma_i + \sigma_j\right), \varepsilon_{ij} = \left(\varepsilon_i \varepsilon_j\right)^{\frac{1}{2}} \quad (4)$$

Each setup included two fragments: open- ended MWCNT or MWSiNT and water molecules. To avoid dealing with asymmetry effect (like the case of non-chiral zigzag structures) the armchair MWNT structures were considered as solute molecules. Armchair-type NTs (5, 5), (6, 6), (7, 7) and (8, 8) were used as the inner walls and the (11, 11) armchair type NT considered as the outer wall.

Since all samples had (11, 11) armchair tube as the outer part, hereafter and all through the manuscript, we referred to the samples only by their inner part characters. For instance, by the (66) pure carbon sample authors mean the sample with the inner tube of (6, 6) and outer tube of (11, 11). The characteristics of the CNT and SiNT water systems were summarized in Table 2. The lengths of the MWNTs were kept constant at 10 Å and diameters were calculated using the following formula

$$d = \frac{a[3(n^2 + nm + m^2)]^{1/2}}{\pi} \quad (5)$$

in which “a” was either the C-C (1.421 Å) or Si-Si (2.410 Å) bond lengths [37].

All calculations were performed in a cubic box at the experimental density of water, 1 g/cm3.

The optimum edges of the box were $50\times50\times50$ Å^3, which corresponded to almost 4000 H2O molecules of pure solvent. In fact a very dilute solution of NTs was used, so one molecule of solute was merged in a cubic box of water and then considering the size of solute (NT) some water molecules were eliminated from the box. Randomly translational and rotational movements for water molecules were considered, too.

The symmetry center of the NT was in the geometrical center of the cell.

Herein, water- carbon LJ interactions were treated within a spherical cutoff. To make a quantitative prediction of the solvation behavior of MWCNTs and MWSiNTs, these kinds of interaction potentials should be treated with more complicated methods such as Ewald summation. However, for the purpose of understanding qualitative aspects of the solvation problem of MWCNTs and MWSiNTs, potentials such as simple LJ terms are sufficiently accurate [38]. Moreover, the interested systems were not highly charged, so in a comparison of typical energy contributions in distance behavior of non-bonded interactions, both short range interactions (Evdw) and long-range ones (Edipole-dipole and Epoint charges) became small in a cutoff between 20-30 Å [39]. Therefore a spherical cutoff for the potential at an OO separation (distance between O atoms of two water molecules) of half the length of an edge of the cube (around 25 Å) seemed reasonable.

During the simulation process, one molecule was picked and displaced randomly on each move. An acceptance rate of 50% for new configurations was achieved by using suitable ranges for translations and rotation about a randomly chosen axis.

Periodic boundary conditions were employed in computation of energy of the initial configuration, in cutoff, in translations and rotations, and computation of the energy of each produced configuration. The system was thoroughly equilibrated using several hundred thousand configurations. The energy of a configuration was obtained from the pair wise sum of the dimerization energies for each monomer, as usual.

In order to find the optimum length of the Markovian chains, we conducted a series of simulations. The outcomes showed that the best length included 5×10^6 configurations since the energy difference between the two last runs (lengths 4×10^6 and 5×10^6) were negligible. For instance the results for (55) pure MWCNT sample are given in Table 3. This procedure was applied to the all samples.

Table 1 Lennard-Jones parameters for carbon and silicon atoms*

Site	ε,kcal/mol	σ,Å	Ref. no.
C	0.080	3.500	33,34
Si	0.310	3.804	35

*ε is the well depth of the interaction potential and σ is the center to center distance when the potential changes from positive to negative

Table 2 Overview of the CNT– and SiNT– water systems*

MWNT	Case	Diameter(Å)	Inter space (Å)	N (C,Si)	N(H_2O)
	55	6.785 (11.507)	8.142 (13.81)	90	3956 (3830)
Inner walls	66	8.142 (13.809)	6.785 (11.508)	108	3958 (3867)
	77	9.499 (16.110)	5.428 (9.207)	126	3960 (3868)
	88	10.856 (18.412)	4.071 (6.905)	144	3968 (3878)
Outer wall	11	14.927 (25.317)		198	

*All systems are aligned in the direction of tube axis. The length of tube is 10 Å and the chirality corresponds to armchair NTs. The space between the inner and outer tube is represented as "inter space". N(C, Si) denotes the number of carbon or silicon atoms in pure samples. The numbers in the parenthesis correspond to SiNTs

Table 3 The optimum length of Markovian chain

No. of runs	10^5	10^6	2×10^6	3×10^6	4×10^6	5×10^6
Energy(kcal/mol)	-8.456	-9.333	-9.357	-9.358	-9.364	-9.363

Roughly 50% of the initial steps were disregarded for equilibrium. Every calculation was extended to include as many configurations as were necessary to reduce the statistical error to the level at which, calculated energy differences have quantitative significance.

The first part of this report studies solvation of pure C and pure Si systems. In the next step, the solvation behavior of several systems comprised of both C and Si in different percentages is investigated. Computation of all probable systems is time consuming and useless. So we studied selected systems with growing percent of Si from the inner tube toward the outer tube in a systematic way. The pure MWCNT was considered as the first structure and then the C atoms in the inner tube were replaced by Si atoms in several steps (each step included replacement of 25% of C atoms) such that in the end we had a MWNT with an inner SiNT and an outer CNT. In the next step we continued to replace C atoms with the same 25% in each step until the final structure which was pure MWSiNT. This sample had only Si in both inner and outer tubes.

Results and discussion

SWNTs always reaggregate over time since this is their thermodynamically favorable state. Therefore, true water-soluble NT solutions are those solutions that entropically favor individualized nanotubes [25, 40], where the reaggregation of CNTs in a solvent is less favored, on a thermodynamic basis, than their continued solvated state [41].

The authors tried to look at the solvation problem from another perspective. Herein, we studied the amount of inner tube water content in terms of tube diameter and tube type (pure C, mixture of C and Si and pure Si). Solvation energies for aforementioned samples were calculated, as well. Finally, comparisons were made between the solvated samples in order to find the optimum solvation conditions.

Solvation of MWNTs; pure CNTs and SiNTs

Calculated solvation energies for MWNTs with different diameters are shown in Fig. 1. As can be seen, for the carbon samples, increasing the diameter of the inner tube has no significant effect on the solvation energies. In other words solvation energies in this case areindependent from the curvature of the inner wall.

MWSiNTs show relatively higher solvation energies (-10 kcal mol^{-1} for MWSiNTs compared to -9 kcal mol^{-1} for C samples). In contrast with pure C samples, solvation energy does not show a smooth trend; it decreases drastically from (66) sample to (77) sample, about 2.5 kcal mol^{-1}, and then it goes up again toward (88) sample (Fig. 1).

There are several arguments on the interactions of NTs in the aqueous solutions. For instance, Frolov et al. study on the solvation behavior of NTs in ionic solutions suggested considering the effect of charge density of the ions and ion's hydration strength on the solubility of the NTs. They also discovered the size of ions as another important point which affects the amount of direct contact with the NT surface [42]. In another study, Striolo et al. used NTs decorated with oxygenated sites (mainly carbonyl groups) to study the solvation behavior of the NT. The result was that the number of CO groups and their distributions were key factors in the solvation of NTs [38].

In our case study we use pure water as solvent and NTs are comprised of C and Si atoms, as solutes. C and Si atoms belong to the same group, but they have different atomic sizes (such as atomic and covalent radii). For instance, C atom has a covalent radius of 70 pm while Si has an amount about 110 pm [43]. Therefore one can come to the idea that the more negative solvation energies of the Si samples are due to their larger size which can provide higher amounts of direct contact between water molecules and NT surface.

The other factor which has to be mentioned is the space between the inner and outer wall of a NT which provides higher capacity of loading material into an MWNT compared with an SWNT. The space between two walls is much bigger in the case of a MWSiNT. It means these tubes are able to keep more water molecules in them which in turn affect their solubility.

As an illustration of the water arrangement around NT, a snapshot issued from the simulation of the (66) MWCNT in water at 298 K is given in Fig. 2, showing the cylindrical symmetry of the water environment near to the NT. This top view picture shows the arrangement of the first, and to a lesser extent the second layer of water molecules around the NT walls.

To understand why the (77) Si sample has the most negative solvation energy it will be insightful to first study the radial distribution functions (RDF).

Distribution functions measure the (average) value of a property as a function of an independent variable. A typical example is the $g(r)$ which measures the probability of finding a particle as a function of distance from a "typical" particle relative to that expected from a completely uniform distribution (i.e., an ideal gas with density N/V), considering that by construction, $g(r)=1$ in ideal gas. Additionally, RDFs are a class of observables properties which characterize the structure of the liquid state. Experimental methods, such as Neutron and X-ray scattering provide information on the so called functions [39, 44, 45]. In the case of NTs, solvent atom type x RDFs, denoted by $g_x(r)$, are obtained from the frequency histogram formula:

$$g_x(r) = \frac{n_x(r)}{(4\pi r^2 dr)\rho_x} \quad (6)$$

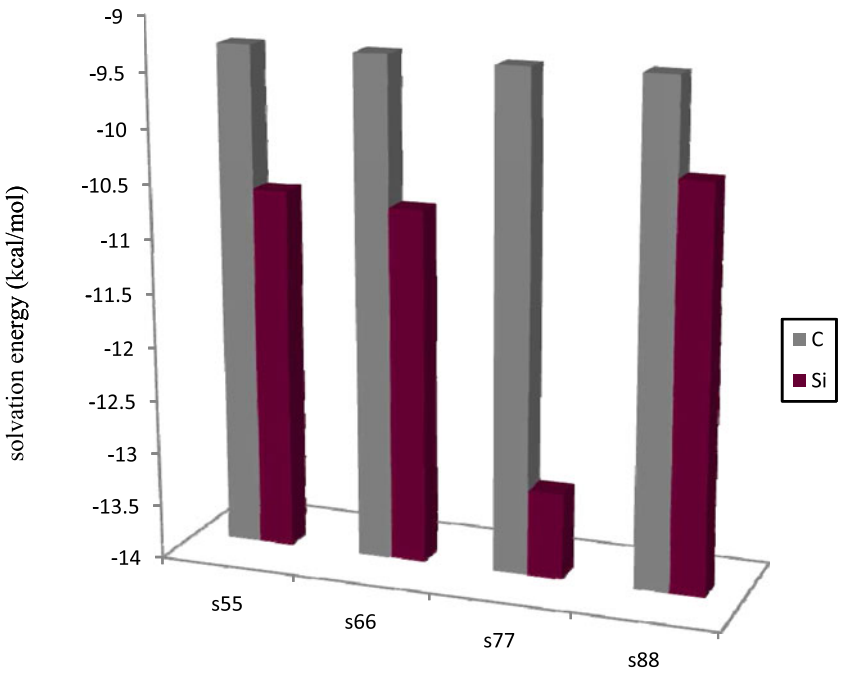

Fig. 1 Solvation energy diagram for pure MWCNT and pure MWSiNT samples with different diameters. MWSiNT (77) appears to be the most soluble one

where "$n_x(r)$" is the frequency of finding an atom of type x (O or H) between r and "$r+dr$" of the central axis of NT , dr is the width of the slab considered from the NT axis to calculate RDF. Finally, ρ_x is the bulk density of atom type x.

Figures 3a, b depict the site –site RDFs for O and H atoms in the inner NT versus (r) axis for pure MWCNTs and MWSiNTs, respectively. Note that the "r" axis corresponds to the distance from the center of the inner tube toward the NT inner wall. Inner tubes are considered with different diameters. In agreement with other reports [46, 47], water density in the NTs strongly depends on the diameter of NT. As can be seen in Fig. 3a, the H atom RDFs for narrower NTs, suggest that H atoms of water molecules face in the interior of the tube and we have one layer of water molecules. The results for (55) and (66) MWCNTs indicate one peak for H atom in about 0.5 Å from the internal axis of NTs, while RDFs of (77) and (88) MWCNTs show two peaks in about 1 Å and 2 Å. So, as the radius of inner tube

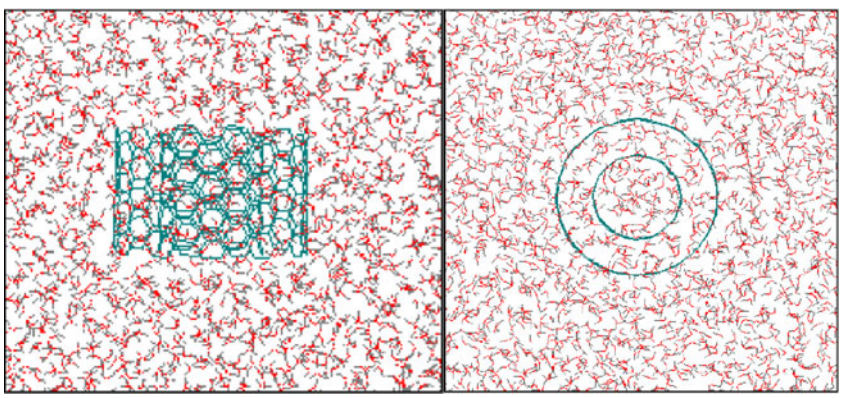

Fig. 2 Snapshot that issued from the simulation of the (66) MWCNT in water: (**a**) side and (**b**) top views of MWCNT in water

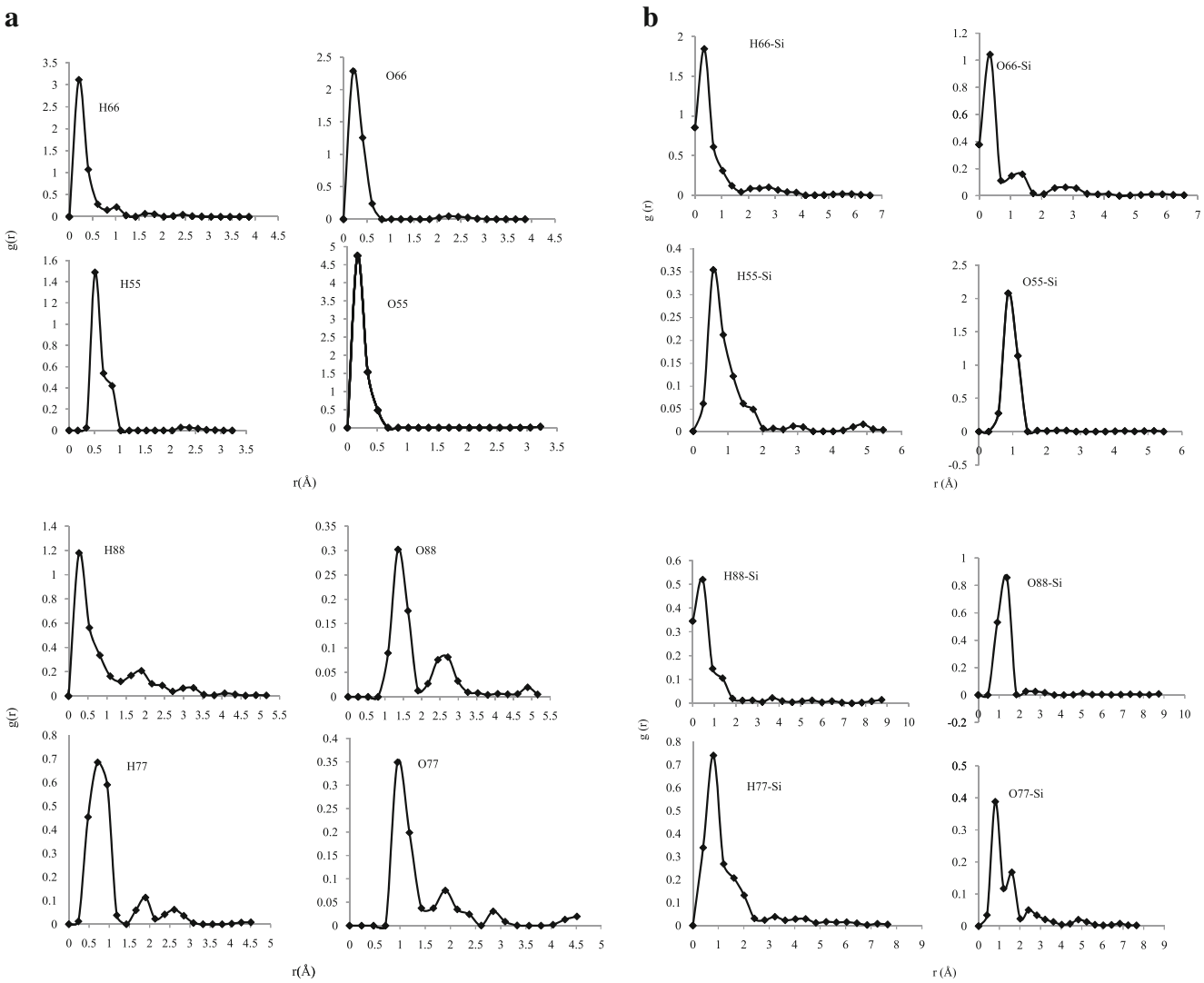

Fig. 3 **a,b**. Site-site RDFs for pure MWCNT and MWSiNT samples

increase, for (77) and (88) MWCNTs, the second layer of H atoms are formed and the first layer moves closer to the walls. This is the characteristic of hydrophobic walls that the H atoms do not move near the edge of tube in the narrower NTs.

RDFs for O atoms in all samples roughly show the same trend. As for the (55) NT sample, a maximum can be seen near the center of the tube (Fig. 3a). For (66) samples with a bigger diameter, this peak moves toward the wall. Eventually, (77) and (88) sample RDFs indicate another maximum which corresponds to a second layer of water molecules in the inner tube. In fact in narrower NTs, we observed one layer of water molecules. As for the (77) and (88) NTs, our results predict the formation of two layers stabilized by hydrogen bonds.

Similar results are obtained for MWSiNTs. However, RDF peaks appear in a wider range from the center of NTs since they have a bigger diameter compared to MWCNTs.

The amount of water molecules between two NTs (inner and outer tubes) represented as local densities. Calculated values for pure C and Si samples are given in Table 4. As can be seen, the limit of bulk water (distances greater than the diameter of the outer wall) is considered, too. In both cases (either C or Si) the local density outside the outer wall is constant and equal to 0.031 and 0.061 for O and H atoms, respectively. It shows the limit of bulk behavior for water.

The local densities in the inner tube (local density<d1) increase as one goes to the larger NTs (either MWCNTs or MWSiNTs). MWSiNTs samples have higher local densities than MWCNTs which corresponds to their larger size. Comparisons between MWCNT(55)-the most insoluble sample- and MWSiNT(77)-which shows the highest solubility- indicate that (55) C sample has the least amount of local density while the (77) Si sample has the most. So, it appears that (77) silicon sample prefers to absorb water molecules rather than pass them through the NT.

Table 4 Calculated local densities (Å-3) for site-site interactions in pure MWCNT and MWSiNT samples *

	55		66		77		88	
			MWCNT samples					
	O	H	O	H	O	H	O	H
local density<d1	0.005	0.01	0.006	0.012	0.01	0.017	0.012	0.025
d1<local density<d2	0.001	0.001	0.003	0.003	0.005	0.006	0.008	0.009
d2<local density	0.031	0.061	0.031	0.061	0.031	0.061	0.031	0.061
			MWSiNT samples					
	O	H	O	H	O	H	O	H
local density<d1	0.002	0.05	0.06	0.11	0.05	0.11	0.03	0.07
d1<local density<d2	0.018	0.017	0.013	0.013	0.022	0.021	0.028	0.027
d2<local density	0.031	0.061	0.031	0.061	0.031	0.061	0.031	0.061

* By definition, local density is the number of particles per volume. d1 and d2 are the diameters of the inner and outer walls, respectively

Also, calculated local densities for H atom in the inner tube and out of the outer tube is higher than the corresponding values of O atom for each sample. This seems reasonable due to the 1:2 ratios of the O/H in water molecule, but in the inter space this ratio is not preserved. Between two layers, the hydrophobic effects of the wall do not provide conditions for normal hydrogen bonding between water molecules. In fact hydrogen bonding is a function of the type of nonstructural space. Hydrogen bonding in the inter space of NTs differ from bulk water. The second hydrogen atom of each adsorbed water molecule does not participate in hydrogen bonds with other adsorbed molecules, but it is instead directed toward the hydrophobic wall. This configuration reproduces the features observed in other reports [48–50]. In this way, the number of hydrogen bonds per water molecule can be significantly less than the number of hydrogen bonds that a water molecule can establish in bulk water. So in the inter space of the NTs, the orientation of water molecules is changed and therefore the O/H ratio of local densities are less than bulk water.

Solvation of mixed multiwall nanotubes

The solvation energies for the two mixed samples (55) and (77) are given in Table 5. The mixing range is considered between 0% (pure state) to 100% for both inner and outer tubes, so the number of total samples in each case is nine. Increasing the Si percentage makes the samples more soluble in both cases. The (55) sample shows a linear relationship between increasing the Si percentage and solubility of the compound (by a regression coefficient of R^2=0.800) while the (77) sample follows a nonlinear form.

To give better description of solubility of mixture NTs, the relative solvation energies (difference between each of the obtained solvation energies to the least of them) are calculated, as well. Figure 4 shows the relative solvation energies (DE) for the mixed (55) and (77) samples. Clearly, the most soluble sample is pure silicon sample (77). The two mixed samples (55) and (77) have the same relative solvation energies at 100%. It means the solubility of the sample in which all the C atoms are replaced by Si atoms in the inner tube, is independent from inner tube diameter. One can see the same situation at 175%, a sample with just 25% of C in its outer wall. On the other hand, the mixed (55) sample shows a higher solubility relative to the mixed (77) when it has 50% Si in its combination in the inner tube. In summary, the obtained energies indicate that the solvation energies of MWNT (55) and (77) in water appears in the following order:

$$E(77)\text{pure Si} > (E55 = E77)175\% > (E55 = E77)100\%$$

Error estimation

There is no denying the fact that a simulation can generate an enormous amount of data that should be properly analyzed to extract relevant properties and to check that the calculation has behaved properly. The three most important factors that determine the accuracy of MC calculations are the quality of intermolecular potentials, the sample size effect, and statistical fluctuations of calculated ensemble

Table 5 Calculated solvation energies (in kcal mol^{-1}) for two samples (55), (77) which were subjected to mixing

	%mixture	E(55)	E(77)
Pure carbon	0	-9.333	-9.367
	25	-9.603	-9.507
	50	-9.647	-9.565
	75	-9.723	-9.788
	100	-9.754	-9.756
	125	-9.891	-9.945
	150	-9.987	-9.962
	175	-10.021	-10.025
Pure silicon	200	-10.755	-13.458

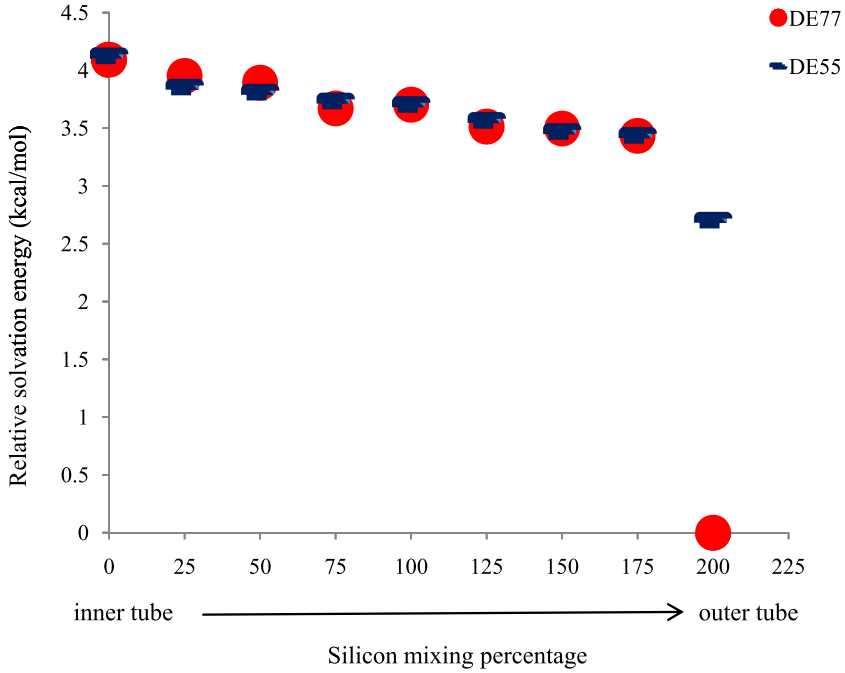

Fig. 4 Calculated relative solvation energies for mixed samples (55) and (77). Explanations: DE77 (in red filled circles) is the relative energy for (77) sample and DE55 (in marine blue line) shows relative solvation energies for (55) sample. (55) and (77) samples have the same relative solvation energies at 100% and 175% . Therefore in these conditions solvation energies are not size dependent

averages. The first was briefly discussed. The second factor arises because locating a limit number of molecules in a box followed by subsequent application of periodic boundary conditions introduces an error into the molecular correlations. For a given system, this effect decreases with the sample size. In most cases of interest, we do not know how to choose the size of the system in order to minimize an effect of periodic boundary conditions.

The most straightforward test is to perform a series of calculations in which the sample size is systematically increased until calculated values remain unchanged. The statistical errors are often reported as standard deviations [45]. The standard deviation and relative errors are tabulated in Table 6.

Conclusions

As dispersed aqueous nanomaterials are used in many applications, making stable solutions of nanomaterials in aqueous phase is an important problem. For this purpose, the effects of size and structural composition on the solvation behavior of MWNTs in water were studied by implementation of the MC computer simulation method.

It was found that variation of the inner tube size has no significant effect on the solubility of the MWCNT samples. Such a trend was not observed in the case of MWSiNTs. For instance, the (77) sample appeared to be the most soluble sample. Investigation of mixed samples revealed that in some certain conditions the solubility behavior became size independent, like an MWNT with just 25% C in its outer wall or an MWNT with a pure Si inner wall and pure C outer wall.

Based on these findings, it seems that MWCNTs are better candidates for transporting water molecules through an MWNT structure, while in the case of water adsorption problems it is better to use MWSiNTs or a mixture of C/Si MWNTs.

The effect of physical conditions such as temperature dependency or pH variations on solubility of these systems, as well as the effect of nonchiral structures, can be of great importance and will be considered in future performances.

Table 6 Simulation errors in terms of standard deviation and relative error for pure MWCNT (55) and MWSiNT (55) samples

Structure	MWCNT			MWSiNT		
	<E>	**STDEV**	**Relative error**	**<E>**	**STDEV**	**Relative error**
55_11	-9.333	0.029	0.003	-10.755	0.223	0.021
66_11	-9.356	0.022	0.002	-10.022	0.010	0.001
77_11	-9.367	0.016	0.002	-13.458	0.300	0.022
88_11	-9.448	0.013	0.001	-10.266	0.005	0.001

References

1. Saupe GB, Waraksa CC, Kim HH, Han YJ, Kaschak DM, Skinner DSM, Mallouk TE (2000) Nanoscale tubules formed by exfoliation of potassium hexaniobate. Chem Mater 12:1556–1562
2. Ozin GA (1992) Nanochemistry: synthesis in diminishing dimensions. Adv Mater 4:612-648
3. Ajayan PM, Stephan O, Colliex C, Trauth D (1994) Aligned carbon nanotube arrays formed by cutting a polymer resin-nanotube composite. Science 265:1212–1214
4. Tans SJ, Devoret MH, Dai H, Thess A, Smalley RE, Geerligs LJ, Dekker C (1997) Individual single-wall carbon nanotubes as quantum wires. Nature 386:474–477
5. Valdes C, Spitz Urs P, Toledo L, Leticia M, Kubik SW, Rebek J Jr (1995) Synthesis and self-assembly of pseudo-spherical homo- and heterodimeric capsules. J Am Chem Soc 117:12733–12745
6. Chen C, Wang X (2006) Adsorption of Ni(II) from aqueous solution using oxidized multiwall carbon nanotubes. Ind Eng Chem Res 45:9144–9149
7. Hilding J, Grulke EA, Sinnott SB, Qian D, Andrews R, Jagtoyen M (2001) Adsorption of butane on carbon multiwall nanotubes at room temperature. Langmuir 17:7540–7544
8. Kalra A, Hummer G, Garde S (2004) Methane partitioning and transport in hydrated carbon nanotubes. J Phys Chem B 108:544–549
9. Ajayan PM (1999) Nanotubes from carbon. Chem Rev 99:1787–1799
10. Venema LC, Wildoer JWG, Janssen JW, Tans SJ, Tuinstra H, Kouwenhoven LP, Dekker C (1999) Imaging electron wave functions of quantized energy levels in carbon nanotubes. Science 283:52–55
11. Son H, Samsonidze GG, Kong J, Zhang Y, Duan X, Zhang J, Liu Z, Dresselhaus MS (2007) Strain and friction induced by van der Waals interaction in individual single walled carbon nanotubes. Appl Phys Lett 90:2531131–2531133
12. Lourie O, Wagner HD (1998) Transmission electron microscopy observations of fracture of single-wall carbon nanotubes under axial tension. Appl Phys Lett 73:3527–3529
13. Teker K, Sirdeshmukh R, Sivakumar K, Lu S, Wickstrom E, Wang HN, Dinh TV, Panchapakesan B (2005) Applications of carbon nanotubes for cancer research. Nanobiotechnology 1:171–182
14. Cuenca AG, Jiang H, Hochwald SN, Delano M, Cance WG, Grobmyer SR (2006) Emerging implications of nanotechnology on cancer diagnostics and therapeutics. Cancer 107:459–466
15. Liu A, Sun K, Yang J, Zhao D (2008) Toxicological effects of multi-wall carbon nanotubes in rats. J Nanopart Res 10:1303–1307
16. Bottini M, Bruckner S, Nika K, Bottini N, Bellucci S, Magrini A, Bergamaschi A, Mustelin T (2006) Multi-walled carbon nanotubes induce T lymphocyte apoptosis. Toxicol Lett 160:121–126
17. Gannon CJ, Cherukuri P, Yakobson BI, Cognet L, Kanzius JS, Kittrell C, Weisman RB, Pasquali M, Schmidt HK, Smalley RE, Curley SA (2007) Carbon nanotube-enhanced thermal destruction of cancer cells in a noninvasive radiofrequency field. Cancer 110:2654–2665
18. Monteiro-Rivierea NA, Nemanichb RJ, Inmana AO, Wangb YY, Rivierea JE (2005) Multi-walled carbon nanotube interactions with human epidermal keratinocytes. Toxicol Lett 155:377–384
19. Kampinga HH (2006) Cell biological effects of hyperthermia alone or combined with radiation or drugs: a short introduction to newcomers in the field. Int J Hyperthermia 22:191–196
20. Zhang Z, Yang X, Zhang Y, Zeng B, Wang S, Zhu T, Roden RBS, Chen Y, Yang R (2006) Delivery of telomerase reverse transcriptase small interfering RNA in complex with positively charged single-walled nanotubes suppresses tumor growth. Clin Cancer Res 12:4933–4939
21. Kam NW, O'Connell M, Wisdom JA, Dai H (2005) Carbon nanotubes as multifunctional biological transporters and near infrared agents for selective cancer cell destruction. PNAS 102:11600–11605
22. Kam NW, Liu Z, Dai H (2005) Functionalization of carbon nanotubes via cleavable disulfide bonds for efficient intracellular delivery of siRNA and potent gene silencing. J Am Chem Soc 127:12492–12493
23. Wenseleers W, Vlasov II, Goovaerts E, Obraztsova ED, Lobach AS, Bouwen A (2004) Efficient isolation and solubilization of pristine single-walled nanotubes in bile salt micelles. Adv Funct Mater 14:1105–1112
24. Hadidi N, Kobarfard F, Nafissi-Varcheh N, Aboofazeli R (2011) Optimization of single-walled carbon nanotube solubility by non-covalent PEGylation using experimental design methods. Int J Nanomedicine 6:737–746
25. Kharisov BI, Kharissova OV, Leija Gutierrez H, Mendez UO (2009) Recent advances on the soluble carbon nanotubes. Ind Eng Chem Res 48:572–590
26. Mavrandonakis A, Froudakis GE, Schnell M, Mulhlhäuser M (2003) From pure carbon to silicon-carbon nanotubes: an ab-initio study. Nano Lett 3:1481–1484
27. Sun XH, Li CP, Wong WK, Wong NB, Lee CS, Lee ST, Teo BK (2002) Formation of silicon carbide nanotubes and nanowires via reaction of silicon (from disproportionation of silicon monoxide) with carbon nanotubes. J Am Chem Soc 124:14464–14471
28. Malek K, Shahimi M (2010) Molecular dynamics simulations of adsorption and diffusionof gases in silicon-carbide nanotubes. J Chem Phys 132:014310-1-10
29. Monajjemi M, Ketabi S, Hashemian Zadeh M, Amiri A (2006) Simulation of DNA bases in water: comparison of the Monte Carlo algorithm with molecular mechanics force fields. Biochemistry (Moscow) 71:S1–S8
30. Metropolis N, Rosenbulth AW, Rosenbulth MN, Teller AH, Teller E (1953) Equation of state calculations by fast computing machines. J Chem Phys 21:1087–1093
31. Allen MP, Tildesley DJ (1987) Computer simulation of liquids. Clarendon Oxford
32. Jorgensen WL, Chandrasekharm J, Madura JD, Impey RW, Klein ML (1983) Comparison of single potential functions for simulating liquid water. J Chem Phys 79:926–935
33. Jorgensen WL (1981) Quantum and statistical mechanical studies of liquids: transferable intermolecular potential functions for water, alcohols, and ethers. Application to liquid water. J Am Chem Soc 103:335–340
34. Jia Y, Wang M, Wu L, Gao C (2007) Separation of CO2/N2 gas mixture through carbon membranes: Monte Carlo simulation. Sep Sci Technol 42:3681–3695
35. Lithoxoos GP, Samios J, Carissan Y (2008) Investigation of silicon model nanotubes as potential candidate nanomaterials for efficient hydrogen storage: a combined *ab initio*/grand canonical Monte Carlo simulation study. J Phys Chem C 112:16725–16728
36. Hansen JP, McDonald IR (1991) Theory of simple liquids. Academic press, London
37. Budyka MF, Zyubina TS, Ryabenko AG, Lin SH, Mebel AM (2005) Bond lengths and diameters of armchair single wall carbon nanotubes. Chem Phys Lett 407:266–271
38. Striolo A, Chialvo AA, Cummings PT, Gubbins KE (2006) Simulated water adsorption in chemically heterogeneous carbon nanotubes. J Chem Phys 124:074710–11
39. Jensen F (2007) Introduction to computational chemistry, 2nd edn. John Wiley and sons Inc
40. Liang F, Billups EW (2007) Water-soluble Single-Wall Carbon Nanotubes as a platform technology for biomedical applications. U.S. Patent 20070110658
41. Tour JM, Hudson JL, Dyke C, Stephenson JJ (2005) Functionalization of carbon nanotubes in acidic media. International Patent WO05113434

42. Frolov AI, Rozhin AG, Fedorov MV (2010) Ion interactions with carbon nanotube surface in aqueous solutions: understanding the molecular mechanisms. Chem Phys Chem 11:2612–2616
43. Cordero B, G´omez V, Platero-Prats AE, Rev´es M, Echeverr´ıa J, Cremades E, Barrag´an F, Alvarez S (2008) Covalent radii revisited. Dalton Trans 2832–2838
44. Frenkel D, Smith B (1996) Understanding molecular simulation. Academic, Dordrecht
45. Leach AR (1996) Molecular modeling: principles and applications. Longman, Essex
46. Striolo A, Chialvo AA, Gubins KE, Cummings PT (2005) Water in carbon nanotubes: adsorption isotherms and thermodynamic properties from molecular simulation. J Chem Phys 122(1-13):234712
47. Hanasaki I, Nakatani A, 1-8 (2006) Hydrogen bond dynamics and microscopic structure of confined water inside carbon nanotubes. J Chem Phys 124:174714
48. Mashl RJ, Joseph S, Aluru NR, Jacobsson E (2003) Anomalously immobilized water: a new water phase induced by confinement in nanotubes. Nano Lett 3:589–592
49. Hummer G, Rasaiah JC, Noworyta JP (2001) Water conduction through the hydrophobic channel of a carbon nanotube. Nature (London) 414:188–190
50. Mann DJ, Halls MD (2003) Water alignment and proton conduction inside carbon nanotubes. Phys Rev Lett 90:195503–195506